Analysis and Measurement of Transducer End Radiation in SAW Filters on Strongly Coupling Substrates

ALI R. BAGHAI-WADJI, MEMBER, IEEE, OSWALD MÄNNER, MEMBER, IEEE, AND RUDI GANß-PUCHSTEIN

Abstract—**We present the analysis and measurement of spurious responses generated at the ends of surface acoustic wave (SAW) interdigital transducers (IDT's). Filters fabricated on $LiNbO_3$ show an unwanted passband ripple whose period indicates additional generation of acoustic waves at the IDT end. As this effect cannot be explained by methods of analysis based on the infinite array approximation, an exact analysis of the complex-valued, frequency-dependent electric charge distribution on the finite IDT structure is required.**

Utilizing the method of moments, our analysis is based on a Green's function concept and a spectral-domain representation. Three effects are shown: The first is the charge accumulation of grounded guard fingers located closely to the IDT end, resulting in unwanted end radiation. The second is acoustic end reflections in split-finger IDT's, occurring at the transition from the periodic finger structure to the free substrate. The third is the finger charge induced by the metallic ground plane when the transducer is driven unbalanced to ground. Computer simulations based on our method agree well with measurements.

I. INTRODUCTION

BASICALLY a SAW filter consists of launching and receiving IDT's. These are comblike thin metallic strips (fingers) deposited on the plane surface of a piezoelectric substrate. The general features of SAW propagation and SAW interaction with IDT fingers are now well understood. Nevertheless, to fulfill the stringent requirements for SAW filters employed in modern telecommunication equipment, it is necessary to understand the mechanisms of the various second-order effects [1], [2], which cause considerable discrepancy between first-order theory and experimental data. As a next step these effects are to be incorporated into the design models and are to be corrected by an iterative design procedure. Among others, the following are the predominant second-order effects: mechanical and electrical reflections in IDT's [3], energy storage effects on SAW propagation in periodic arrays [4], influence of external matching on phase and amplitude response, transducer end effects and neighbor coupling effects [5], [6], transversal end effects in SAW IDT's [7], [8], coupling to electromagnetic waves and acoustic bulk waves [9]–[13], losses due to the finite resistivity of the fingers [14], [15], surface wave diffraction and beam steering [16], the waveguiding effect in SAW-IDT's, and losses due to surface roughness of the piezoelectric substrate. Some of these effects are still subjects of active research.

The present paper for the first time discusses three second-order effects, which can be observed if a SAW IDT with a finite number of fingers is deposited on the surface of a piezoelectric substrate with a metallized grounded back plane.

The SAW filter substrate must be neither too thin (fragile) nor too thick because this leads to excessive electromagnetic feedthrough and economically is unsound (typical wafer thickness, 500 μm). To suppress electromagnetic cross talk between the input and output IDT, a SAW filter is usually mounted in a shielding metal casing. Conductive (silver loaded) adhesives are often used to coat the backside of the crystal substrate and to mount it in its housing. Due to the finite dimension of the substrate the time-domain response of the device depends on the IDT driving arrangement (upper or lower pad driven with respect to ground, Figs. 3 and 4).

Filters fabricated on $LiNbO_3$ show an unwanted passband ripple whose period indicates additional generation of acoustic waves at the IDT end. As this effect cannot be explained by methods of analysis based on the infinite array approximation [17], an exact analysis of the complex-valued, frequency-dependent electric charge distribution on the finite IDT structure is required [18]–[20]. The latter can be regarded as the distributed source of the excitation of acoustic waves due to the corresponding Coulomb forces in the piezoelectric crystals [21].

In the following, based on a Green's function concept [9], [25] (for a theoretical treatment see, for example, [22]–[24]), a spectral-domain representation [26]–[28], and the method of moments (MoM) [29]–[31], an efficient formalism [6], [8], [19], [32]–[34] for the calculation of the spatial charge density distribution will be presented.

Manuscript received January 28, 1988; revised June 24, 1988. This work was supported by Siemens AG, Central Research Laboratories, Munich, West Germany, and by the Austrian Science Research Fund under Project 5311.

A. R. Baghai-Wadji is with the Institut für Allgemeine Elektrotechnik und Elektronik, Technische Universität Wien, A-1040 Vienna, Austria.

O. Männer is with Electronic Development, Siemens AG Österreich, A-1100 Vienna, Austria.

R. Ganß-Puchstein is with the Central Research Laboratory, Siemens AG, München, West Germany.

IEEE Log Number 8824259.

0018-9480/89/0100-0150$01.00 ©1989 IEEE

In treating linear boundary value problems, as is well known, the primary task is the construction of a Green's function, which is the response of the medium under consideration to a Dirac δ excitation (line-, point-source excitation). Generally, the construction of Green's function is a difficult procedure. Using spectral-domain representation, the determination of Green's function in the wavenumber domain can be simplified considerably. In this way the governing system of linear differential equations in conjunction with the imposed boundary conditions is transformed into a linear system of algebraic equations. A simple elimination procedure reveals a relation between the spectral components of the source and the response functions. From the latter, by inspection, Green's function in the wavenumber domain can be found.

In the wavenumber domain many interesting facts can be deduced from the functional behavior of Green's function. As we will demonstrate below, Green's function will or will not have a pole singularity at the origin, depending on whether or not the line charge source, which excites the medium, is *isolated*. (If at a finite distance from an assumed line charge source a grounded, unbounded metallic body does not exist, the line source may be called *isolated*. Otherwise it is a *nonisolated* one.) Simple pole singularity, say at $k = k_0$, represents a surface wave, while a branch point singularity at $k = k_b$ characterizes a volume wave (bulk wave excitation is not treated in this paper).

However, a problem arises: the resulting Green's function in the wavenumber domain must be transformed into the real space. This is a difficult procedure, which inherently is accompanied by integral transform techniques. From a computational point of view, it is more efficient in some cases to perform the inverse Fourier transform of the product of Green's function in the wavenumber domain and Fourier transform of the source distribution, which excites the medium. The advantages of this technique will be extensively discussed in Section II.

As we will discuss below, the Green's function constructed for our boundary value problem consists of two parts, a purely electrostatic part and a second part, which describes the SAW propagation on the surface of a semi-infinite anisotropic piezoelectric substrate. In the wavenumber domain both components are given in closed form. In the real space, the SAW part can be derived analytically, while for the electrostatic part, in its general form, there is no closed-form representation. However, in the special case where the permittivity of the substrate material is much higher than that of free space, the electrostatic component can also be derived analytically.

The constructed Green's function is a good approximation if the predominant acoustic wave is a Rayleigh wave. Nevertheless, the method discussed here is not restricted to Rayleigh wave excitation problems only. A proper extension of Green's function discussed here allows the calculation of IDT interaction with both surface and bulk acoustic waves [12], [13]. Moreover, employing the same method of analysis, the diffraction problem of acoustic waves excited by arbitrary finite structures on piezoelectric media can be analyzed efficiently [12], [13].

In what follows, first, using Green's function in the spectral domain and the inverse Fourier transform, an integral relation for the potential distribution on the surface of the substrate is established. Then, employing the MoM, the associated integral representation is reduced to a matrix equation. In this way the SAW components of the elements of the involved matrix are evaluated analytically. The solution of the resulting linear system of equations yields an approximation for the charge distribution. From the latter all the relevant characteristics of the SAW IDT can be derived in analytical form. A fairly simple modification of the aforementioned matrix makes it possible to include in the analysis the single and interconnected floating fingers with arbitrary geometrical complexity [6], [32]. It must be emphasized that, from a computational point of view, the main advantage of the present method is the possibility of deriving nearly all of the occurring formulas in closed form, so that the time-consuming numerical evaluation of the Fourier transform is avoided.

This paper is organized as follows. In Section II the basic relations are established and the proposed solution procedure is outlined. Section III deals with a discussion of the Green's function for our boundary value problem. In Section IV, based on a nonequidistant discretization of the fingers, a step function approximation of the charge density distribution on the fingers is formulated. In section V the MoM is applied to our problem. A simple expression for the input power of a SAW IDT is derived in Section VI.

In Section VII simulation results based on our theory are compared with experimental data. Three effects will be discussed. The first is the charge accumulation on grounded guard fingers located close to the IDT end, resulting in unwanted end radiation. The second is acoustic end reflections in split-finger IDT's, occurring at the transition from the periodic finger structure to the free substrate. The third is the finger charge induced by a metallic grounded back plane when the transducer is driven unbalanced to ground.

Several SAW filters consisting of unapodized split-finger IDT's with varying numbers of guard fingers have been fabricated. The frequency response has been measured and transformed into the time domain, where the different effects of interest can be observed separately. The calculated time response of the devices is in good agreement with measurements.

II. Theory

Assume N_f infinitely thin metallic fingers with ideal conductivity deposited in parallel fashion on the plane surface of a piezoelectric substrate of finite thickness D. The finger geometry and the finger potentials may be arbitrary. The back side of the substrate may be metallized and grounded (Fig. 1). The problem is to find an efficient method for the analysis of the frequency-dependent spatial charge density distribution. Once the charge distribution on the fingers has been calculated, all the relevant IDT parameters, such as the total capacitance, the input admittance, and, consequently, the insertion loss, can be uniquely determined [9]–[13].

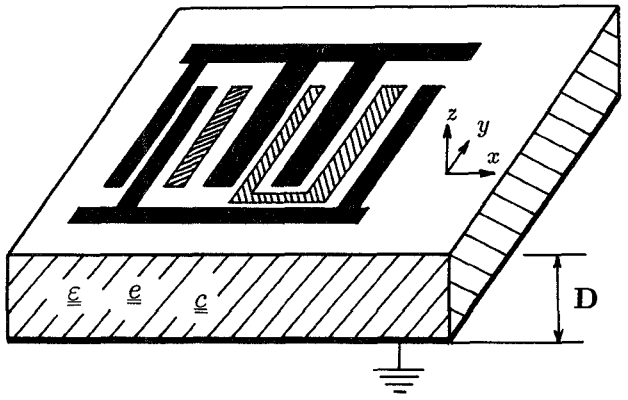

Fig. 1. SAW IDT on the surface of a piezoelectric substrate of finite thickness with grounded back plane.

The linearity of the boundary value problem sketched in Fig. 1 implies the validity of the superposition principle. Equivalent to the latter property is the fact that the potential on the surface of the substrate, $\Phi(x)$, can be written as a convolution integral:

$$\Phi(x) = \int_{-\infty}^{+\infty} G(x'-x)\rho(x')\,dx' \tag{1}$$

where $\rho(x)$ is the spatial charge density distribution and $G(x)$ is the Green's function characterizing the boundary value problem shown in Fig. 1. By definition, $G(x)$ is the potential distribution on the surface of the substrate if an infinitely long line charge source in the y direction located at $x = 0$ excites the medium. A time dependence according to $e^{j\omega t}$ is assumed. As will be discussed below, for the problem sketched in Fig. 1 the Green's function and consequently the charge distribution depend on the angular frequency ω. Keeping in mind that for each frequency value the charge distribution must be evaluated individually, in (1) the variable ω has been omitted.

Remark

Actually, in the above boundary value problem, the potential response of the medium to a line charge source is a two-dimensional function, $G(x, z)$. Now, what is the reason for referring to $G(x)$ with the property $\lim_{z\to 0} G(x, z) = G(x)$ as the Green's function? This is due to the fact that the distributed source, which controls the electric potential (electric field) distribution, is located on the fingers, which reside in the interface and possess given potential values. Therefore we have to construct an expression for the potential distribution on the surface and match (relate) it to the given potential values of the fingers, if the variable x passes the finger regions. Consequently, for the problem treated here, only the electrical conditions on the surface of the substrate must be understood.

Following the ideas of Milsom *et al.* [9] (they considered a line charge source excitation of a semi-infinite piezoelectric substrate) and disregarding the excitation of bulk acoustic waves, $G(x)$ can be decomposed into two parts:

$$G(x) = G^e(x) + G^{\mathrm{SAW}}(x). \tag{2}$$

$G^e(x)$ and $G^{\mathrm{SAW}}(x)$ are, respectively, the electrostatic and the SAW component of Green's function. Insertion of (2) into (1) yields

$$\Phi(x) = \Phi^{(1)}(x) + \Phi^{(2)}(x) \tag{3}$$

with

$$\Phi^{(1)}(x) = \int_{-\infty}^{+\infty} G^e(x'-x)\rho(x')\,dx' \tag{4}$$

and

$$\Phi^{(2)}(x) = \int_{-\infty}^{+\infty} G^{\mathrm{SAW}}(x'-x)\rho(x')\,dx'. \tag{5}$$

An equivalent formula for $\Phi^{(1)}(x)$ is

$$\Phi^{(1)}(x) = \frac{1}{2\pi}\int_{-\infty}^{+\infty} \bar{G}^e(k_x)\bar{\rho}(k_x)e^{-jk_x x}\,dk_x. \tag{6}$$

(Convolution in configuration space corresponds to multiplication in the wavenumber space [35].) The bar indicates Fourier transform.

For the following reason we will use (6) instead of (4) for $\Phi^{(1)}(x)$. Equation (4) demands the determination of the Green's function in real space. Apart from some simple cases, generally it is not possible to transform the Green's function from the wavenumber domain into real space in closed form. The associated Fourier integrals must be evaluated numerically. Calculating these oscillating integrals, the behavior of $\bar{G}^e(k_x)$ for large and small values of k_x will be of importance. As will be shown in the next section for $k_x \gg 1$, we have $\bar{G}^e(k_x) \sim 1/k_x$ ($\sim$ symbolizes asymptotically equal to). Now, if we use a step function approximation for the charge density distribution on the fingers we obtain $|\bar{\rho}(k_x)| \sim 1/k_x$. Thus for $k_x \gg 1$ the relation $\bar{G}^e(k_x)|\bar{\rho}(k_x)| \sim 1/k_x^2$ is valid. Using a triangle function approximation for the charge density distribution we have $\bar{G}^e(k_x)|\bar{\rho}(k_x)| \sim 1/k_x^3$. Therefore, comparing Fourier integral representations

$$G(x) = 1/2\pi \int_{-\infty}^{+\infty} \bar{G}^e(k_x)e^{-jk_x x}\,dk_x$$

and

$$\Phi^{(1)}(x) = 1/2\pi \int_{-\infty}^{+\infty} \bar{G}^e(k_x)\bar{\rho}(k_x)e^{-jk_x x}\,dk_x$$

for Green's function and for the potential distribution on the surface, respectively, the following can be concluded: For $k_x \gg 1$ the integral expression for $\Phi^{(1)}(x)$ shows a better convergence behavior than the integral representing $G(x)$. Further, for problems where $\bar{G}^e(k_x)$ is singular at $k_x = 0$, we have $\bar{\rho}(0) = \lim_{k_x\to 0} \int_{-\infty}^{+\infty}\rho(x)e^{jk_x x}\,dx = \int_{-\infty}^{+\infty}\rho(x)\,dx = 0$, which is the condition for charge conservation. Therefore, $\bar{G}^e(k_x)\bar{\rho}(k_x)$ in (6) is regular at $k_x = 0$. (In cases where $\bar{G}^e(k_x)$ is regular at $k_x = 0$ there is no difficulty at all.) From these we conclude that the integrand in (6) is always a well-behaved function for both $k_x \ll 1$ and $k_x \gg 1$.

With regard to (3), (5), and (6), and following the concept described in [6], [8], [12], [13], [18], [19], and [32]–[34], the following solution procedure can be outlined.

Solution Procedure

i) Derive the expression for $\bar{G}^e(k_x)$.
ii) Construct an expression for $\bar{G}^{SAW}(k_x)$.
iii) Determine the inverse Fourier transform of $\bar{G}^{SAW}(k_x)$.
iv) Discretize the fingers (nonequidistantly) in N_s strips.
iv) Using suitable basis functions, construct a sum approximation for $\rho(x)$ and from that a sum approximation for $\bar{\rho}(k_x)$.
vi) Insert $\bar{G}^e(k_x)$ and the approximation for $\bar{\rho}(k_x)$ in (6), interchange the order of summation and integration, and evaluate (numerically) the involved integrals. The resulting expression is an approximation for $\Phi^{(1)}(x)$.
vii) Insert $G^{SAW}(x)$ and the approximation for $\rho(x)$ in (5), interchange the order of summation and integration, and evaluate the involved integrals (in closed form). The resulting expression is an approximation for $\Phi^{(2)}(x)$.
viii) Equation (3) together with (5) and (6) yields an approximation for $\Phi(x)$, the potential distribution on the surface of the substrate.
ix) Choose appropriate weighting functions.
x) Define an inner product for two complex-valued functions.
xi) Apply MoM to $\Phi(x)$. This leads to a system of N_s equations for N_s unknown charge values on the N_s strips.

In what follows, for $\bar{G}^e(k_x)$ and $G^{SAW}(x)$, respectively, we will use our previously published results [33] and the approximation given by Milsom *et al.* [9].

III. Green's Function

In the preceding section the results of the Green's function concept were presented in a general form. Attention is now turned to an approximation to the general theory. Here we will discuss the expressions for the aforementioned two components of the Green's function. First, we will discuss the properties of the electrostatic component of the Green's function in the wavenumber domain and then the SAW component of the Green's function both in the wavenumber domain and in the configuration space.

A. Electrostatic Component of Green's Function

In [33] we have shown that $\bar{G}^e(k_x)$ has the functional form

$$\bar{G}^e(k_x) = \frac{1}{\epsilon_0 |k_x|} \frac{1}{1 + \epsilon_{P,r} \coth\left(\frac{\epsilon_{P,r}}{\epsilon_{33,r}} D|k_x|\right)} \tag{7}$$

with

$$\epsilon_{P,r} = \sqrt{\epsilon_{11,r}\epsilon_{33,r} - \epsilon_{13,r}^2},$$

where $\epsilon_{P,r}$ is the effective relative permittivity constant for the anisotropic substrate in Fig. 1. D is the thickness of the substrate. $\bar{G}^e(k_x)$ is an overall regular function, with the following properties:

1) The first concerns the behavior of $\bar{G}^e(k_x)$ in the limit $D \to \infty$. In this limit the line charge source on the substrate surface is no longer shielded by a grounded plane at a finite distance. The line source becomes *isolated*. In this case for a SAW IDT on the surface, the charge neutrality condition must be met; i.e., $(\bar{\rho}(0) =) \int_{-\infty}^{+\infty} \rho(x)\, dx = 0$. Denoting Green's function for the semi-infinite substrate by $\bar{G}_\infty^e(k_x)$ and introducing the parameter $\alpha_e = 1/\epsilon_0 \cdot (1 + \epsilon_{P,r})$, then from (7) we have

$$\bar{G}_\infty^e(k_x) = \frac{\alpha_e}{|k_x|}. \tag{8}$$

As is known, the expression on the right-hand side is the Green's function for a semi-infinite anisotropic substrate, with the characteristic pole singularity at $k_x = 0$. In real space, if we interpret the inverse Fourier integral of (8) in Cauchy's sense, we obtain

$$G_\infty^e(x) = -\frac{\alpha_e}{\pi}\gamma - \frac{\alpha_e}{\pi} \lim_{\epsilon \to 0} \ln\epsilon - \frac{\alpha_e}{\pi} \ln|x| \tag{9}$$

where γ is Euler's constant. Inserting (9) into (4), with regard to the charge neutrality condition, get

$$\Phi_\infty^{(1)}(x) = -\frac{\alpha_e}{\pi} \int_{-\infty}^{+\infty} \ln|x' - x| \rho(x')\, dx'. \tag{10}$$

Note that the pole singularity in $\bar{G}_\infty^e(k_x)$ results in the divergent term $\lim_{\epsilon \to 0} \ln\epsilon$, which only in connection with the charge conservation condition leads to a physically meaningful expression for $\Phi_\infty^{(1)}(x)$.

2) The second property concerns the behavior of $\bar{G}^e(k_x)$ in the limit $k_x \to 0$: $\lim_{k_x \to 0} \bar{G}^e(k_x) = D/(\epsilon_0 \epsilon_{33,r}) = \text{const.}$ In contrast to Green's function of the semi-infinite substrate, (eq. (8)), $\bar{G}^e(k_x)$ is regular at $k_x = 0$. This is because the line charge source, which excites the medium, is shielded by the grounded plate (*nonisolated line charge source*).

3) For the special case where the permittivity of the substrate material is much higher than that of free space ($\epsilon_{P,r} \gg 1$) we find the following approximate formula for $\bar{G}^e(k_x)$:

$$\bar{G}^e(k_x) \approx \frac{1}{\epsilon_0} \frac{1}{1 + \epsilon_{P,r}} \frac{1}{|k_x|} \tanh\left(\frac{\epsilon_{P,r}}{\epsilon_{33,r}} D|k_x|\right). \tag{11}$$

The inverse Fourier transform of (11) can be carried out analytically [36], yielding

$$G^e(x) \approx \frac{1}{\pi\epsilon_0} \frac{1}{1 + \epsilon_{P,r}} \ln\left(\coth\left(\frac{\pi}{4} \frac{\epsilon_{33,r}}{\epsilon_{P,r}} \frac{|x|}{D}\right)\right). \tag{12}$$

B. SAW Part of Green's Function

Up to this point we have entirely neglected the piezoelectric property of the substrate. To include this effect, we use an approximation for the SAW component of the Green's function discussed by Milsom *et al.* [9]. This approximation will be based on the assumption that the predominant surface acoustic wave is a Rayleigh wave. In

addition, we shall assume that the bulk acoustic waves are not excited. Therefore, while for the electrostatic part of the Green's function we have taken into account the finite thickness of the substrate, constructing the SAW part we may assume that the piezoelectric substrate is a semi-infinite medium. The validity of this approach for the frequency range of interest is established by comparing calculated results with experimental data (Section VII).

Milsom *et al.* [9] have shown that, for a semi-infinite piezoelectric substrate, the SAW part of the Green's function $\bar{G}^{\mathrm{SAW}}(k_x)$ can be written as

$$\bar{G}^{\mathrm{SAW}}(k_x) = \frac{2k_0 G_s}{k_x^2 - k_0^2}. \tag{13}$$

G_s is a piezoelectric coupling factor and k_0 is the wavenumber at the free surface of the substrate for a Rayleigh wave propagating with velocity v_0 at frequency ω. An expression analogous to (13) can be obtained directly if the propagation of a disturbance caused by a Dirac δ force on a infinitely long string with uniform mass density is considered.

Using (13) and applying Cauchy's residue theorem, Milsom *et al.* have shown that the resulting Green's function for a line charge source located at $x = 0$ is

$$G^{\mathrm{SAW}}(x) = -jG_s e^{-jk_0|x|} \tag{14}$$

(remember a time dependence according to $e^{j\omega t}$ has been assumed). Taking the magnitude of x in the exponential term ensures the propagation of outgoing waves only. The negative sign in the exponent is due to the positive sign in the exponent of $e^{j\omega t}$. As k_0 is proportional to ω, $G^{\mathrm{SAW}}(x)$ depends on frequency.

IV. Approximation of the Charge Density

Assume that the fingers have already been discretized into N_s strips. (To emphasize the logarithmic singularity of the electrostatic part of the charge density at finger edge points, the strips at the finger ends are chosen to be narrower than the strips in the middle region of the fingers. In the following, ξ_l^m and δ_l, respectively, denote the midpoint coordinate and one half of the width of the lth strip; x_l^b and x_l^e, respectively, are the start and end point coordinates of the lth strip.

Employing MoM, most commonly impulse, pulse, or triangle functions are used as basis functions. The following analysis will be based on pulse functions; i.e.,

$$\rho(x) = \sum_{l=1}^{N_s} \rho_l \cdot P_l(x) \tag{15}$$

where

$$P_l(x) = \begin{cases} 1 & \text{if } x_l^b \leqslant x \leqslant x_l^e \\ 0 & \text{otherwise} \end{cases} \tag{16}$$

with $\int_{-\infty}^{+\infty} P_l(x)dx = x_l^e - x_l^b$. The quantity ρ_l denotes the constant unknown charge density value on the lth strip. We now replace the unknown charge density values ρ_l by the corresponding charge density integrals, i.e., by the strip charges $q_l = \rho_l(x_l^e - x_l^b)$. As a result we have

$$\rho(x) = \sum_{l=1}^{N_s} q_l \cdot \frac{1}{(x_l^e - x_l^b)} P_l(x). \tag{17}$$

Because of the nonequidistant discretization of the fingers, this, from a computational point of view, is an important step. While the terms q_l are approximately of the same order of magnitude, the values of ρ_l can differ by many orders of magnitude. On the other hand, taking q_l as the unknowns becomes necessary if we try to obtain a symmetric matrix as a final result (eq. (29)).

The Fourier transform of $\rho(x)$ can be carried out directly, giving

$$\bar{\rho}(k_x) = \sum_{l=1}^{N_s} q_l \frac{1}{(x_l^e - x_l^b)} \frac{e^{jk_x x_l^e} - e^{jk_x x_l^b}}{jk_x}. \tag{18}$$

V. Potential Distribution on the Surface

As mentioned above, the potential at the surface can be written as the sum of the two components $\Phi^{(1)}(x)$ and $\Phi^{(2)}(x)$. At this stage of calculation we have to establish an appropriate inner product, denoted by $\langle u, v \rangle$. In this context, in the theory of MoM, a frequently used inner product of two complex-valued functions $u(x)$ and $v(x)$ is defined as

$$\langle u, v \rangle = \int_{-\infty}^{+\infty} u(x) v^*(x)\, dx \tag{19}$$

where the asterisk denotes the complex conjugate. Next, we have to choose proper weighting functions. As in the case with basic functions, usually impulse, pulse, or triangle functions are used as weighting functions. In the present analysis, we will use pulse functions $P_k(x)$.

For a nonequidistant discretization (as in our case), it is necessary to use a modified form of (19) (normalized weighting functions). Applying this to $\Phi(x)$ we obtain

$$\varphi_k = \frac{\int_{-\infty}^{+\infty} \Phi(x) P_k(x)\, dx}{\int_{-\infty}^{+\infty} P_k(x)\, dx}. \tag{20}$$

($P_k(x)$ is a real-valued function; therefore we have $P_k^*(x) = P_k(x)$.) The quantity φ_k is the potential applied to the kth strip. Inserting (3) into (20) together with $\int_{-\infty}^{+\infty} P_k(x)\, dx = x_k^e - x_k^b$ yields

$$\varphi_k = \varphi_k^{(1)} + \varphi_k^{(2)} \tag{21}$$

with

$$\varphi_k^{(i)} = \frac{1}{(x_k^e - x_k^b)} \int_{x_k^b}^{x_k^e} \Phi^{(i)}(x)\, dx \qquad (i = 1,2). \tag{22}$$

Here $\varphi_k^{(1)}$ and $\varphi_k^{(2)}$ are the contributions to the potential of the kth strip arising from $G^e(x)$ ($\bar{G}^e(k_x)$) and $G^{\mathrm{SAW}}(x)$, respectively.

With regard to (22), in the next four calculation steps we will formulate approximations for $\Phi^{(1)}(x)$, $\varphi_k^{(1)}$, $\Phi^{(2)}(x)$, and, finally, $\varphi_k^{(2)}$.

Approximation for $\Phi^{(1)}(x)$

Insertion of (18) into (6) and subsequent interchange of the order of summation and integration yield

$$\Phi^{(1)}(x) = \sum_{l=1}^{N_s} q_l \frac{1}{(x_l^e - x_l^b)} \frac{1}{2\pi} \times \int_{-\infty}^{+\infty} \bar{G}^e(k_x) \frac{e^{jk_x(x_l^e - x)} - e^{jk_x(x_l^b - x)}}{jk_x} dk_x. \quad (23)$$

Approximation for $\varphi_k^{(1)}$

Insertion of the above equation into (22), rearrangement of the order of summation and integration, and calculation of the integrals over x yield

$$\varphi_k^{(1)} = \sum_{l=1}^{N_s} q_l \cdot I_{kl}^{(1)} \qquad (k = 1, \cdots, N_s) \quad (24a)$$

with

$$I_{kl}^{(1)} = \frac{1}{\pi} \int_0^{\infty} \bar{G}^e(k_x) \cdot \operatorname{sinc}(\delta_k k_x) \cdot \operatorname{sinc}(\delta_l k_x) \cdot \cos(k_x |\xi_k^m - \xi_l^m|)\, dk_x. \quad (24b)$$

Deriving $I_{kl}^{(1)}$ we have used the property that $\bar{G}^e(k_x)$ is an even function of k_x. With regard to (7) this condition is met. Generally, for problems where the reciprocity condition holds, this property remains valid.

Remarks

1) $I_{kl}^{(1)}$ is symmetric with respect to the indices k and l; i.e. $I_{kl}^{(1)} = I_{lk}^{(1)}$. This property results from the reciprocity relations (symmetric Green's function), the fact that we have chosen the same functions (pulse functions) for the basis as well as for the weighting functions, and, finally, the fact that we have replaced the unknowns ρ_l by the corresponding q_l.

2) In the limit $D \to \infty$; i.e., in the case of a semi-infinite substrate, $I_{kl}^{(1)}$ can be calculated analytically:

$$I_{kl}^{(1)} = \frac{1}{\pi\epsilon_0(1+\epsilon_{P,r})} \cdot \frac{1}{(x_k^e - x_k^b)(x_l^e - x_l^b)} \cdot \Big[+ (x_k^b - x_l^b)^2 \cdot \ln|x_k^b - x_l^b| - (x_k^b - x_l^e)^2 \cdot \ln|x_k^b - x_l^e| - (x_k^e - x_l^b)^2 \cdot \ln|x_k^e - x_l^b| + (x_k^e - x_l^e)^2 \cdot \ln|x_k^e - x_l^e| \Big]. \quad (25)$$

3) For $k \neq l$ the oscillation of the integrand in (24b) mainly is given by $|\xi_k^m - \xi_l^m|$ in the argument of the cosine function. (For $k \neq l$ we have $|\xi_k^m - \xi_l^m| > \delta_k, \delta_l$.) If k equals l, then the integrand oscillates according to $\sin^2(\delta_l k_x)$.

Approximation for $\Phi^{(2)}(x)$

Insertion of the approximation for $\rho(x)$ (eq. (17)) and $G^{\mathrm{SAW}}(x)$ (eq. (14)) into (5), interchange of the order of summation and integration, and calculation of the resulting integrals lead to

$$\Phi^{(2)}(x) = \sum_{l=1}^{N_s} q_l I_l^{(2)}(x) \quad (26a)$$

with

$$I_l^{(2)}(x) = \frac{G_s}{k_0(x_l^e - x_l^b)} \cdot \begin{cases} \left[+ e^{-jk_0(x_l^e - x)} - e^{-jk_0(x_l^b - x)} \right] & \text{if } x \leqslant x_l^b (< x_l^e) \\ \left[-2 + e^{-jk_0(x_l^e - x)} + e^{jk_0(x_l^b - x)} \right] & \text{if } x_l^b \leqslant x \leqslant x_l^e \\ \left[- e^{jk_0(x_l^e - x)} + e^{jk_0(x_l^b - x)} \right] & \text{if } (x_l^b <) x_l^e \leqslant x. \end{cases} \quad (26b)$$

Approximation for $\varphi_k^{(2)}$

Inserting (26a) into (22), interchanging the order of summation and integration, and evaluating the associated integrals, we obtain

$$\varphi_k^{(2)} = \sum_{l=1}^{N_s} q_l \cdot I_{kl}^{(2)} \qquad (k = 1, \cdots, N_s) \quad (27a)$$

with

$$I_{kl}^{(2)} = \begin{cases} -jG_s e^{-jk_0|\xi_k^m - \xi_l^m|} \cdot \operatorname{sinc}(\delta_k k_0) \cdot \operatorname{sinc}(\delta_l k_0) & \text{if } k \neq l \\ \dfrac{G_s}{\delta_l k_0} \left[-1 + e^{-jk_0\delta_l} \cdot \operatorname{sinc}(\delta_l k_0) \right] & \text{if } k = l. \end{cases} \quad (27b)$$

Notice the symmetry property of $I_{kl}^{(2)}$ with respect to the indices k and l; i.e., $I_{kl}^{(2)} = I_{lk}^{(2)}$.

Now, having calculated the approximate expressions for $\varphi_k^{(1)}$ and $\varphi_k^{(2)}$, the evaluation of φ_k is straightforward. Equation (21) together with (24a) and (27a) yields

$$\varphi_k = \sum_{l=1}^{N_s} q_l A_{kl} \qquad (k = 1, \cdots, N_s) \quad (28)$$

where $A_{kl} = I_{kl}^{(1)} + I_{kl}^{(2)}$. The $I_{kl}^{(1)}$ and $I_{kl}^{(2)}$ are both symmetric. Hence we have $A_{kl} = A_{lk}$. Equation (28) in matrix form reads

$$\underline{\varphi} = \underline{\underline{A}} \cdot \underline{q}. \quad (29)$$

Thus, we have derived a relation between the given potentials of the fingers and the unknown charge values on the strips. Solution of the matrix equation (29) results in the charge density integrals, which depend on the frequency. The frequency dependence manifests itself in k_0 according to (27b).

The matrix $\underline{\underline{A}}$ can be extended in a simple manner to include in the analysis single and/or blocks of interconnected floating fingers. The procedure is the same as we have already discussed for purely electrostatic problems in semi-infinite media [6], [32]. Floating fingers can be analyzed simultaneously with neighbor active fingers, and no iteration steps are required.

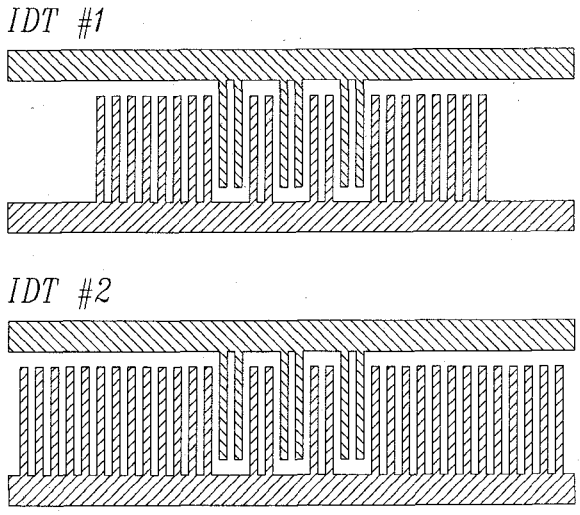

Fig. 2. IDT geometries of filters #1 and #2.

VI. Input Power of a SAW IDT

The electrical input power for any SAW transducer of uniform finger length W is given by

$$P_{\text{in}} = \frac{1}{2} W \cdot \text{Re} \int_{-\infty}^{+\infty} \Phi(x) i^*(x)\, dx \tag{30}$$

where the current density $i(x)$ is defined as $i(x) = j\omega\rho(x)$. Substituting $i(x)$ into (30) yields

$$P_{\text{in}} = \frac{1}{2} \omega W \cdot \text{Im} \int_{-\infty}^{+\infty} \Phi(x) \rho^*(x)\, dx. \tag{31}$$

Inserting (15) into (31) and interchanging the order of summation and integration, with regard to (20) and with the definition $q_l = \rho_l(x_l^e - x_l^b)$ we obtain

$$P_{\text{in}} = \frac{1}{2} \omega W \cdot \text{Im} \sum_{l=1}^{N_s} \varphi_l q_l^*. \tag{32}$$

VII. Experimental Results and Simulations

Two SAW filters #1 and #2, consisting of two unweighted split finger IDT's, were fabricated and measured. The IDT's consisting of six active overlaps had a center frequency of 140 MHz and an aperture of 3000 μm. In addition to the active fingers, filters #1 and #2, respectively, had at the left and right sides six and 11 dummy fingers (see Fig. 2). These fingers are usually added to the active region of an IDT to approximate an infinite periodic grating, for which in the case of a semi-infinite substrate a closed-form formula for the charge distribution is available [17].

The measurement range was from 45 to 235 MHz and included the main lobe and the nearest sidelobes of the $\sin(x)/x$ transfer function. For a better discrimination of the second-order effects involved, the data were transformed into the time domain (Figs. 3 and 4).

The trailing peaks marked by arrows in Figs. 3 and 4 result from IDT end reflections. While reflections cancel within the IDT because of the $\lambda/4$ spaced fingers, this is not the case at the ends. This is due to the fact that the

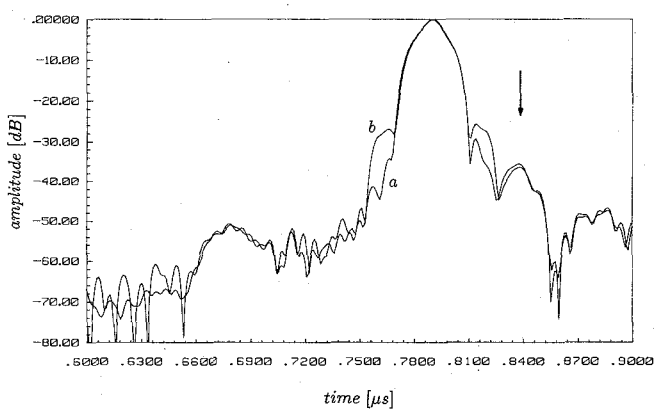

Fig. 3. Measured time-domain response of filter #1. (a) Upper pad driven, "grounded" dummy fingers. (b) Lower pad driven, "hot" dummy fingers.

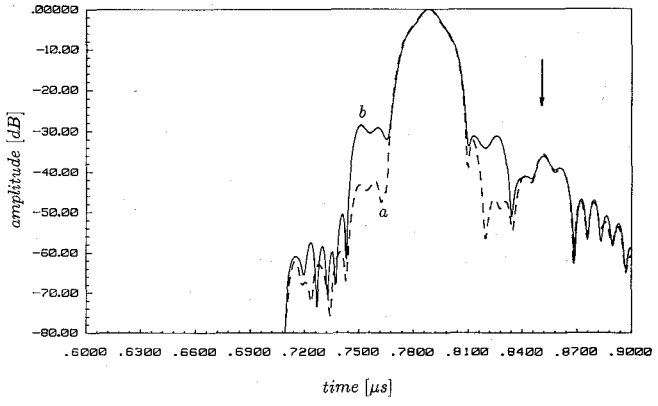

Fig. 4. Measured time-domain response of filter #2. (a) Grounded dummy fingers. (b) Hot dummy fingers.

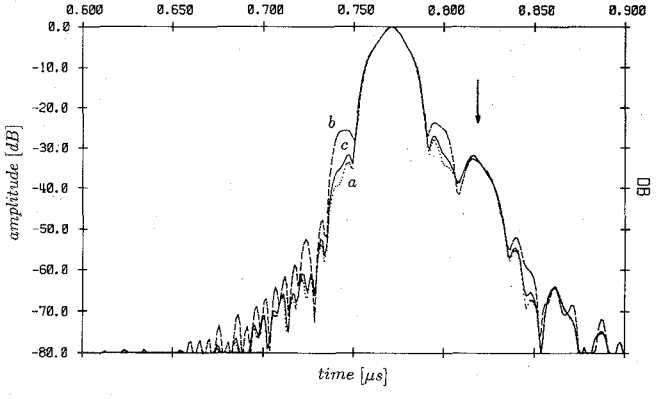

Fig. 5. Calculated time-domain response of filter #1. (a) Grounded dummy fingers. (b) Hot dummy fingers. (c) Semi-infinite substrate.

reflectivity of a single finger at the end of the IDT is different from the reflectivity of a finger within the IDT. This effect cannot be predicted by models based on the cascading of identical three-port unit cells [37], whose parameters are obtained from an infinite array analysis.

To demonstrate the versatility of the presented method, we have calculated (Figs. 5 and 6) the time response of #1 and #2, respectively, for the following two cases: curves (a) with the dummy fingers grounded and curves (b) with excited dummy fingers. For comparison, we have also

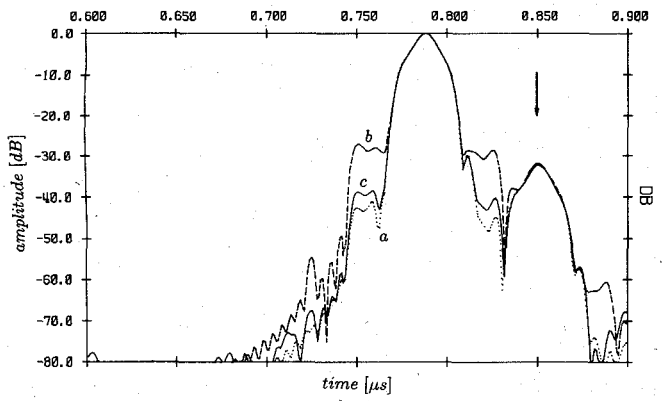

Fig. 6. Calculated time-domain response of filter #2. (a) Grounded dummy fingers. (b) Hot dummy fingers. (c) Semi-infinite substrate.

included the time response of the IDT on a substrate with infinite thickness (curves (c) in Figs. 5 and 6). The pedestals appearing for case (b) at both sides of the main response are due to charge accumulation on the "hot" dummy fingers induced by the presence of the grounded back plane. The arrows mark reflections from the IDT ends.

The calculated time response of the devices is in good agreement with the measurements.

VIII. Conclusion

Employing the method of moments and the concept of the Green's function in conjunction with the spectral-domain representation, an efficient semianalytical method for the analysis of SAW interaction with IDT's has been presented. Nearly all of the occurring formulas have been derived in closed form. The influence of end fingers as well as the influence of a grounded metal back plane on the charge distribution has been simulated by means of this method. Theoretically and experimentally, three second-order effects in SAW IDT's are shown. The first is the charge accumulation on grounded guard fingers located close to the IDT end, resulting in unwanted end radiation. The second is acoustic end reflections in split-finger IDT's. The third is the influence of the metal ground plane on the charge distribution when the transducer is driven unbalanced to ground. Good agreement between computer simulations and experimental results is achieved.

Acknowledgment

Many comments and helpful discussions with Prof. F. Seifert and Dr. M. Kowatsch are gratefully appreciated. Special thanks are due to Dr. G. Riha for continuous encouragement and support.

References

[1] W. Stanley Jones, C. S. Hartmann, and T. D. Strurdivant, "Second order effects in surface wave devices," *IEEE Trans. Sonics Ultrason.*, vol. SU-19, pp. 368–377, July 1972.

[2] H. Skeie and H. Engan, "Second-order effects in acoustic surface-wave filter design methods," *Radio Electron. Eng.*, vol. 45, pp. 207–220, May 1975.

[3] H. Skeie, "Mechanical and electrical reflections in interdigital transducers," in *Proc. 1972 IEEE Ultrason. Symp.*, pp. 335–337.

[4] S. Datta and B. J. Hunsinger, "An analysis of energy storage effects on SAW propagation in periodic arrays," *IEEE Trans. Sonics Ultrason.*, vol. SU-27, pp. 333–341, Nov. 1980.

[5] C. S. Hartmann and B. G. Secrest, "End effects in interdigital surface wave transducers," in *Proc. 1972 IEEE Ultrason. Symp.*, pp. 413–416.

[6] A. R. Baghai-Wadji, S. Selberherr, and F. Seifert, "On the calculation of charge, electrostatic potential and capacitance in generalized finite SAW structures," in *Proc. 1984 IEEE Ultrason. Symp.*, pp. 44–48.

[7] R. S. Wagers, "Transverse electrostatic end effects in interdigital transducers," in *Proc. 1976 IEEE Ultrason. Symp.*, pp. 536–539.

[8] A. R. Baghai-Wadji, S. Selberherr, and F. Seifert "Rigorous 3D electrostatic field analysis of SAW transducers with closed-form formulae," in *Proc. 1986 IEEE Ultrason. Symp.*, pp. 23–28.

[9] R. F. Milsom, N. H. Reilly, and M Redwood, "Analysis of generation and detection of surface and bulk acoustic waves by interdigital transducers," *IEEE Trans. Sonics Ultrason.*, vol. SU-24, pp. 147–166, May 1977.

[10] A. M. Hussein and V. M Ristic, "The evaluation of the input admittance of SAW interdigital transducers," *J. Appl. Phys.*, vol. 50, no. 7, pp. 4794–4801, July 1979.

[11] V. M. Ristic and A. M. Hussein, "Radiation pattern of bulk modes from a finite interdigital transducer on $Y-Z$ $LiNbO_3$," *IEEE Trans. Sonics Ultrason.*, vol. SU-27, pp. 15–21, Jan. 1980.

[12] K. C. Wagner, G. Kovacs, A. R. Baghai-Wadji, and F. Seifert, "Analysis of interdigital transducer interaction with SAW and BAWs," in *Proc. 1987 IEEE Ultrason. Symp.*, pp. 149–153.

[13] F. Seifert, A. R. Baghai-Wadji, K. C. Wagner, and G. Kovacs, "Calculation of interdigital transducer interaction with SAW and BAWs," to be published in *Proc. 1988 European Mechanics Colloq. 226: Nonlinear and Other Non-Classical Effects in Surface Acoustic Waves*.

[14] K. M. Lakin, "Electrode resistance effects in interdigital transducers," *IEEE Trans. Microwave Theory Tech.*, vol. MTT-22, pp. 418–424, 1974.

[15] O. Männer, E. Ehrmann-Falkenau, and H. Stocker, "Analysis of electrode resistance effects in SAW filters on strongly coupling substrates," in *Proc. 1984 IEEE Ultrason. Symp.*, pp. 77–81.

[16] M. S. Kharusi and G. W. Farnell, "Diffraction and beam steering for surface-wave comb structures on anisotropic substrates," *IEEE Trans. Sonics Ultrason.*, vol. SU-18, pp. 35–42, 1971.

[17] H. Engan, "Excitation of elastic surface waves by spatial harmonics of interdigital transducers," *IEEE Trans. Electron Devices*, vol. ED-16, pp. 1014–1017, 1969.

[18] A. R. Baghai-Wadji, "Closed-form formulae analysis of SAW interaction with arbitrary interdigital transducer structures," in *Proc. 1986 Surface Waves in Solids and Layered Structures Symp.*, (USSR), pp. 214–217.

[19] A. R. Baghai-Wadji, O. Männer, S. Selberherr, and F. Seifert, "Analysis and measurement of transducer end radiation in SAW filters on strongly coupling substrates," in *Proc. 1987 1st European Frequency and Time Forum*, (France), pp. 315–319.

[20] O. Männer, A. R. Baghai-Wadji, E. Ehrmann-Falkenau, and R. Ganss, "Mixed nodal variable/scattering parameter formalism for the analysis of SAW transducers," in *Proc. 1987 European Conf. Circuit Theory and Design* (France), pp. 669–674.

[21] B. A. Auld, *Acoustic Fields and Waves in Solids*. New Nork: Wiley, 1973, vol. 2, pp. 170–177.

[22] G. F. Roach, *Green's Functions*. Cambridge: Cambridge University Press, 1967.

[23] R. P. Kanval, *Generalized Functions*. New York: Academic Press (mathematics in science and engineering), vol. 171, 1983, pp. 217–243.

[24] I. Stackgold, *Green's Functions and Boundary Value Problems*. New York: Wiley, 1979.

[25] D. P. Morgan, *Surface Wave Devices for Signal Processing*. Amsterdam: Elsevier, 1985, pp. 39–80.

[26] T. Itoh and A. S. Herbert, "A generalized spectral domain analysis for coupled suspended microstriplines with tunning septums," *IEEE Trans. Microwave Theory Tech.*, vol. MTT-26, pp. 820–826, Oct. 1978.

[27] T. Itoh, "Generalized spectral domain method for multiconductor printed lines and its application to turnable suspended microstrips," *IEEE Trans. Microwave Theory Tech.*, vol. MTT-26, pp. 983–987, Dec. 1978.

[28] T. Itoh and R. Mittra, "A technique for computing dispersion characteristics of shielded microstriplines," *IEEE Trans. Microwave Theory Tech.*, vol. MTT-22, pp. 896–898, Oct. 1974.

[29] R. F. Harrigton, *Field Computation by Moment Method*. New York: Macmillan, 1968.

[30] R. F. Harrigton, "Matrix methods for field problems," *Proc. IEEE*, vol. 55, pp. 136–149, Feb. 1967.

[31] M. M. Nye, "Method of moments as applied to electromagnetic problems," *IEEE Trans. Microwave Theory Tech.*, vol. MTT-33, pp. 972–980, 1985.

[32] A. R. Baghai-Wadji, S. Selberherr, and F. Seifert, "Closed-form electrostatic field analysis for metallic comb-like structures containing single and interconnected floating strips of arbitrary topological complexity, Part I: One-dimensional representation; Part II: Two-dimensional representation," in *Proc. 1986 IGTE Symp.*, (Austria), pp. 138–145 and pp. 146–153.

[33] ____, "A Green's function approach to the electrostatic problem of single, coupled and comb-like metallic structures in anisotropic multilayered media," in *Proc. 1986 AMSE*, vol. 2.1, (Italy), pp. 109–120.

[34] ____, "Two-dimensional Green's function of a semi-infinite anisotropic dielectric in the wavenumber domain," *IEEE Trans. Ultrasonics Ferroelectrics Frequency Control*, vol. UFFC-33, pp. 315–317, May 1986.

[35] D. C. Champeney, *Fourier Transforms and their Physical Applications*. London: Academic Press, 1973.

[36] I. S. Gradshteyn and I. M. Ryzhik, *Table of Integrals, Series and Products*. New York: Academic Press, 1980, pp. 516, formula 4.116-2.

[37] C. Panasik and B. Hunsinger, "Scattering matrix analysis of surface acoustic wave reflectors and transducers," *IEEE Trans. Sonics Ultrason.*, vol. SU-28, pp. 79–91, 1981.

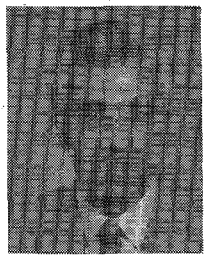

Ali R. Baghai-Wadji (M'88) was born in Marand, Iran, on May 6, 1953. He received the Dipl. Ing. degree in communication engineering from the Vienna University of Technology, Austria, in 1984.

In 1980 he joined the Institut für Allgemeine Elektrotechnik und Elektronik at the Technical University of Vienna, where he was engaged in the analysis of surface acoustic wave devices. Since 1984 he has been a Research Assistant. His doctoral thesis was on the calculation of source distribution for the excitation of acoustic waves in piezoelectric media. He received the Dr. Techn. degree at the same university in 1987. His areas of scientific interest include the radiation and scattering of piezoelectric and electromagnetic waves, and the development and application of numerical and analytical methods for the analysis and design of piezoelectric, electromagnetic, and electro-optic devices.

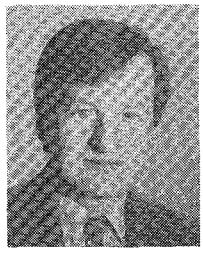

Oswald Männer (M'85) was born in Vienna, Austria, on October 2, 1958. He received the Dipl. Ing. and Dr. Techn. degrees in electrical engineering from the Technical University of Vienna in 1983 and 1987, respectively.

From 1983 to 1987 he was with the Institut für Allgemeine Elektrotechnik und Elektronik at the Technical University of Vienna, where he was engaged in the numerical simulation of surface acoustic wave devices. In 1987, he joined the process and device modeling group at the Siemens AG Österreich in Vienna, where he continues to work on SAW device simulation.

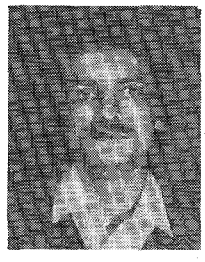

Rudi Ganß-Puchstein was born in Schoenenberg, West Germany, on September 28, 1957. He received the Diploma in electrical engineering at the University of Kaiserslauten, West Germany, in 1985.

Since 1985 he has been in the Corporate Research and Development Division of Siemens AG in Munich. From 1985 to 1987, he was responsible for the development of spectrum shaping SAW filters for digital radio relay systems. Since 1987, he has been working on tools for the development of SAW filters.